Dependence of positive and negative sprite morphology on lightning characteristics and upper atmospheric ambient conditions

Jianqi Qin, Sébastien Celestin, Victor P. Pasko

▶ **To cite this version:**

Jianqi Qin, Sébastien Celestin, Victor P. Pasko. Dependence of positive and negative sprite morphology on lightning characteristics and upper atmospheric ambient conditions. Journal of Geophysical Research Space Physics, 2013, 118 (5), pp.2623-2638. 10.1029/2012JA017908 . insu-01291206

HAL Id: insu-01291206
https://insu.hal.science/insu-01291206

Submitted on 20 May 2016

HAL is a multi-disciplinary open access archive for the deposit and dissemination of scientific research documents, whether they are published or not. The documents may come from teaching and research institutions in France or abroad, or from public or private research centers.

L'archive ouverte pluridisciplinaire **HAL**, est destinée au dépôt et à la diffusion de documents scientifiques de niveau recherche, publiés ou non, émanant des établissements d'enseignement et de recherche français ou étrangers, des laboratoires publics ou privés.

JOURNAL OF GEOPHYSICAL RESEARCH: SPACE PHYSICS, VOL. 118, 2623–2638, doi:10.1029/2012JA017908, 2013

Dependence of positive and negative sprite morphology on lightning characteristics and upper atmospheric ambient conditions

Jianqi Qin,[1] Sebastien Celestin,[1,2] and Victor P. Pasko[1]

Received 4 May 2012; revised 29 November 2012; accepted 30 November 2012; published 22 May 2013.

[1] Carrot sprites, exhibiting both upward and downward propagating streamers, and columniform sprites, characterized by predominantly vertical downward streamers, represent two distinct morphological classes of lightning-driven transient luminous events in the upper atmosphere. It is found that positive cloud-to-ground lightning discharges (+CGs) associated with large charge moment changes (Qh_Q) tend to produce carrot sprites with the presence of a mesospheric region where the electric field exceeds the value $0.8E_k$ and persists for $\gtrsim 2$ ms, whereas those associated with small Qh_Q are only able to produce columniform sprites. Columniform sprites may also appear in the periphery of a sprite halo produced by +CGs associated with large Qh_Q. For a sufficiently large Qh_Q, the time dynamics of the Qh_Q determines the specific shape of the carrot sprites. In the case when the sufficiently large Qh_Q is produced mainly by an impulsive return stroke, strong electric field is produced at high altitudes and manifests as a bright halo, and the corresponding conductivity enhancement lowers/enhances the probability of streamer initiation inside/below the sprite halo. A more impulsive return stroke leads to a more significant conductivity enhancement (i.e., a brighter halo). This conductivity enhancement also leads to fast decay and termination of the upper diffuse region of carrot sprites because it effectively screens out the electric field at high altitudes. On the contrary, if the sufficiently large Qh_Q is produced by a weak return stroke (i.e., a dim halo) accompanied by intense continuing current, the lightning-induced electric field at high altitudes persists at a level that is comparable to E_k, and therefore an extensive upper diffuse region can develop. Furthermore, we demonstrate that 'negative sprites' (produced by -CGs) should be necessarily carrot sprites and most likely accompanied by a detectable halo, since the initiation of upward positive streamers is always easier than that of downward negative streamers, and -CGs are usually associated with impulsive return stroke with no continuing current. We also conjecture that in some cases, fast decaying single-headed upward positive streamers produced by -CGs may appear as bright spots/patches. We show that the threshold charge moment changes of positive and negative sprites are, respectively, ~320 and ~500 C km under typical nighttime conditions assumed in this study. These different initiation thresholds, along with the different applied electric field required for stable propagation of positive and negative streamers and the fact that +CGs much more frequently produce large charge moment changes, represent three major factors in the polarity asymmetry of +CGs and -CGs in producing sprite streamers. We further demonstrate that lower mesospheric ambient conductivity leads to smaller threshold charge moment change required for the production of carrot sprites. We suggest that geographical and temporal conductivity variations in the lower ionosphere documented in earlier studies, along with the seasonal and inter-annual variations of thunderstorm activity that lead to different lightning characteristics in the troposphere, account for the different morphological features of sprites observed in different observation campaigns.

Citation: Qin, J., S. Celestin, and V. P. Pasko (2013), Dependence of positive and negative sprite morphology on lightning characteristics and upper atmospheric ambient conditions, *J. Geophys. Res. Space Physics, 118*, 2623–2638, doi:10.1029/2012JA017908.

[1]Communications and Space Sciences Laboratory, Department of Electrical Engineering, Penn State University, University Park Pennsylvania, USA.
[2]Now at Laboratory of Physics and Chemistry of the Environment and Space (LPC2E), National Center for Scientific Research (CNRS), Observatory of Sciences of the Universe in the French Center region (OSUC), University of Orleans, Orleans Cedex 2, France.

Corresponding author: Jianqi Qin, Communications and Space Sciences Laboratory, Department of Electrical Engineering, Penn State University, University Park, Pennsylvania, USA. (juq108@psu.edu)

©2012. American Geophysical Union. All Rights Reserved.
2169-9380/13/2012JA017908

1. Introduction

[2] Upper atmospheric gas discharges known as sprites [*Sentman et al*., 1995] are the most morphologically complex type of transient luminous events (TLEs) induced by intense lightning activity in the underlying thunderstorms [*Lyons*, 1996]. Observations have shown that sprite forms can be as simple as a single short vertical column about 10 km long, less than 1 km in diameter, and showing little or no brightness variation along its length [e.g., *Wescott et al*., 1998; *Adachi et al*., 2004], or can be composed of many distinct, spatially separated filaments with a complex mixture of sizes, orientations and shapes that usually extend from ~90 km down to ~40 km altitude [e.g., *Stanley et al*., 1999; *Gerken et al*., 2000; *Stenbaek-Nielsen et al*., 2000]. Moreover, these sprites with extensive vertical structures are sometimes preceded or accompanied by a brief descending diffuse glow with lateral extent 40-70 km, centered at ~80 km altitude, and referred to as a sprite halo [*Barrington-Leigh et al*., 2001; *Wescott et al*., 2001].

[3] Sprites are generally classified into columniform sprites and carrot sprites based on their resemblance to straight columns or carrots in normal-rate ($\lesssim$1000 fps) video observations [*Pasko et al*., 2011, and references therein]. It should be noted that these phenomenological terminologies misrepresent somewhat the streamer nature of the sprite tendrils and instead, depict a "frozen history" of the fast movement of very small and bright volumes of intense ionization in streamer heads [*Marshall and Inan*, 2006]. Recently, imaging of sprites at 5000-10,000 fps has provided significant details of spatial and temporal development of sprite streamers [e.g., *Cummer et al*., 2006; *McHarg et al*., 2007; *Stenbaek-Nielsen and McHarg*, 2008]. In the context of the 10,000 fps observations, columniform sprites are reinterpreted as sprites without any significant upward propagating streamers, whereas carrot sprites have both downward and upward streamers [*Stenbaek-Nielsen and McHarg*, 2008].

[4] Simultaneous video observations of sprites and electromagnetic measurements of lightning radiation indicated that the morphological features of sprites were closely related to the characteristics of their causative positive cloud-to-ground (+CG) lightning discharges [e.g., *Wescott et al*., 1998]. *Adachi et al*. [2004] analyzed the columniform sprite events observed in the Hokuriku area of Japan in the winter of 2001/2002 and documented that 16 out of 22 (73%) events were produced by +CGs associated with charge moment changes $Qh_Q \lesssim$ 500 C km, and six other events were associated with larger Qh_Q up to 1200 C km. It is of interest to note that Japanese winter sprites have much simpler structure than those in the Japanese summer and U.S. continental events, and usually are produced by +CGs associated with Qh_Q of ~200-700 C km [*Hayakawa et al*., 2004]. More recently, *van der Velde et al*. [2006] suggested that the in-cloud lightning activity following the causative +CG and contributing to the continuing current plays an important role in the generation of carrot sprites but appears to be relatively unimportant for columniform sprites. These authors conjectured that carrot sprites are produced by larger total charge moment changes, whereas columniform sprites are produced by larger instantaneous charge moment changes during a +CG discharge [*van der Velde et al*., 2006]. Similarly, *Suzuki et al*. [2011] suggested that sprite-producing lightning discharges with continuing current accompanied by relatively large multiple peaks with ELF waveforms tend to generate carrot sprites, and those with transient currents tend to produce columniform sprites.

[5] Although lightning characteristics seem to be of essential importance to account for the morphological complexity of sprites, it has been questioned whether some other parameters, such as atmospheric conditions leading to the lightning activity, or the electrical properties of the ambient atmosphere, are also controlling the sprite morphology [*Stenbaek-Nielsen et al*., 2010]. This question has been raised as a result of an analysis on the basis of a high-speed imaging dataset obtained during 10 years of sprite observations [*Stenbaek-Nielsen et al*., 2010] where it was found that the relative numbers and morphological features of sprites vary significantly from campaign to campaign. It was stated by *Stenbaek-Nielsen et al*. [2010] that "For example, in 1999 we observed many very big sprite events, "jellyfish" [*Stenbaek-Nielsen et al*., 2000], but these have been rare in later observations. Also in 1999 almost half of the events were halos only; in the recordings 2005–2008 there have been very few halos. In the 2007 campaign most of the sprites were multiple C sprites, but in 2008 most were carrot sprites. In 2005 most sprites started with C sprite characteristic and some developed into carrot sprites."

[6] Recent modeling efforts on sprite streamer inception mechanism have provided new insights in the understanding of sprite morphology [*Qin et al*., 2011, 2012a]. *Qin et al*. [2011] discussed the relations of sprite halo and sprite streamers, and indicated that a sprite halo was a large-scale response of the lower ionosphere as a multiple-avalanche system to the charge removal from thundercloud by a lightning discharge. Its diffuse glow is an optical manifestation of the large-scale conductivity enhancement by electron impact ionization during the transient process of dielectric relaxation of the lightning-induced electric field, whereas sprite streamers are initiated from competing electron density inhomogeneities, which are strong enough to rapidly build up a large space charge field and transform into streamers before relaxation of the external field [*Qin et al*., 2011]. *Qin et al*. [2012a] further investigated streamer formation in different regions of a sprite halo, and found that single-headed (unidirectional) and double-headed (bidirectional) streamers, or secondary upward negative streamers are initiated in different sub-regions of the streamer initiation region (SIR). This difference stems from the ambient conductivity dependence on altitude and the modification of the conductivity by sprite halos, that leads to different dielectric relaxation time in different parts of the halo, corresponding to regions of single-headed streamer initiation (single-SIR) and double-headed streamer initiation (double-SIR).

[7] On the basis of the subdivision into single and double-headed SIRs, it appears that absence or presence of the double-headed SIR is essential for the production of columniform or carrot sprites, respectively, in a sprite-halo event [*Qin et al*., 2012a]. The investigation of the impact of lightning characteristics and the lower ionospheric ambient conditions on the formation of the double-headed SIR represents a major goal of the present work. Furthermore, although *Qin et al*. [2011] predicted that the upper part of 'negative sprites' (produced by -CGs) dominated by positive streamers should be brighter than the lower part dominated

by negative streamers, in agreement with observations of *Taylor et al*. [2008] and *Li and Cummer* [2011], the morphology of these 'negative sprites' has not yet been analyzed in the existing literature. Hence, a theoretical understanding of the morphological features of negative sprites and their more stringent initiation requirements compared to those of positive sprites represents another important goal of the present work.

2. Model

[8] A two-dimensional (2D) cylindrically symmetric plasma fluid model is used to simulate the dynamics of sprite halos and sprite streamers. Most of the model is identical to that used by *Qin et al*. [2012a] except that in the present work, we include the following electron detachment process:

$$O^- + N_2 \rightarrow e + N_2O \tag{1}$$

that appears to be important for long timescale ($\gtrsim$10 ms) dynamics of sprite halos [*Liu*, 2012] and may play a role in the initiation of long-delayed sprites [*Luque and Gordillo-Vazquez*, 2012]. The rate constant κ_d of the reaction (1) is taken from the work of *Rayment and Moruzzi* [1978, Figure 4]. Other reactions that are commonly considered in previous plasma fluid modeling of sprites include:

$$e + N_2 \rightarrow 2e + N_2^+ \tag{2}$$

$$e + O_2 \rightarrow 2e + O_2^+ \tag{3}$$

$$e + O_2 \rightarrow O + O^- \tag{4}$$

Reactions (2) and (3) are the production of electrons via electron impact ionization of N_2 and O_2 molecules, and reaction (4) is the loss of electrons due to dissociative attachment to molecular oxygen.

[9] Although the inclusion of reaction (1) represents an improvement when compared to the model used by *Qin et al*. [2012a], this model may still not be able to accurately simulate the sprite halo dynamics during 10s to 100s of milliseconds, as it ignores many reactions that are important on long timescales [*Sentman et al*., 2008; *Gordillo-Vazquez*, 2008]. Nevertheless, in our simulations we observe that on a 5 ms timescale considered in the present work, the detachment process only slightly affects the mesospheric electric field $\vec{E}_{\mathrm{halo}}(r,z,t)$ in sprite halos [*Gordillo-Vazquez*, 2008; *Liu*, 2012]. This is because there are no ambient O^- ions in our modeling [*Gordillo-Vazquez*, 2008; *Liu*, 2012] and the space charge distribution is not significantly changed by the detachment processes within 5 ms. We ignored other even slower chemical reactions, such as three-body detachment, electron-ion and ion-ion recombination, that are not important on a 5 ms timescale [e.g., *Gordillo-Vazquez*, 2008; *Sentman et al*., 2008; *Liu*, 2012]. We note that this 5 ms timescale is long enough to study the properties of short-delayed sprites [*Cummer and Lyons*, 2005], and to account for important lightning characteristics such as the dramatic contrasts in the durations of continuing currents in +CGs and -CGs [*Williams et al*., 2012].

[10] In this model, we distinguish charged species as electrons, positive ions, O^- ions and ambient negative ions. The ambient positive and negative ions contribute to the total conductivity only by drift motion since we assume that they are not involved in any chemical reactions as reactants over a 5 ms timescale, and O^- ions are produced via reaction (4) and release electrons via reaction (1). The motion of charged species is simulated by solving the drift-diffusion equations for electrons and ions coupled with Poisson's equation:

$$\frac{\partial n_e}{\partial t} + \nabla\cdot\left(n_e \vec{v}_e - D_e \nabla n_e\right) = (\nu_i - \nu_a) n_e + \kappa_d n_{N_2} n_{O^-} + S_{ph} \tag{5}$$

$$\frac{\partial n_p}{\partial t} + \nabla\cdot n_p \vec{v}_p = \nu_i n_e + S_{ph} \tag{6}$$

$$\frac{\partial n_n}{\partial t} + \nabla\cdot n_n \vec{v}_n = 0 \tag{7}$$

$$\frac{\partial n_{O^-}}{\partial t} + \nabla\cdot n_{O^-} \vec{v}_{O^-} = \nu_a n_e - \kappa_d n_{N_2} n_{O^-} \tag{8}$$

$$\nabla^2 \varphi = -\frac{q_e}{\varepsilon_0}\left(n_p - n_e - n_n - n_{O^-}\right) \tag{9}$$

where n_e, n_p, n_n, n_{O^-} and n_{N_2} are, respectively, the electron, positive ion, ambient negative ion, O^- ion and molecular nitrogen number densities; $\vec{v}_e$, $\vec{v}_p$, $\vec{v}_n$ and $\vec{v}_{O^-}$ are the drift velocities of electrons, positive ions, ambient negative ions and O^- ions, respectively. We note that the initial values of n_e, n_p, and n_n are respectively equal to the ambient electron, ambient positive ion, and ambient negative ion densities in the lower ionosphere, which will be introduced in the following using equation (11). S_{ph} is the rate of electron-ion pair production due to photoionization; φ is the electric potential, and ε_0 is the permittivity of free space. The electron drift velocity is defined as $\vec{v}_e = -\mu_e \vec{E}$, where $\vec{E} = -\nabla\varphi$ is the electric field, and the drift of ions is incorporated assuming the mobility of all ion species as a function of altitude $\mu_i \simeq 2.3 N_0/N$ cm^2/V/s [*Davies*, 1983], where N is the air density at the altitude of interest and $N_0 \simeq 2.688\times10^{25}$ m^{-3} is a reference value of air density at the ground level. The electron mobility μ_e, diffusion coefficient D_e, and the ionization ν_i and two-body attachment ν_a frequencies are defined as functions of the reduced electric field E/N using modified formulations of *Morrow and Lowke* [1997]. The transport equations for charged species are solved using a flux-corrected transport technique [*Zalesak*, 1979] that combines an eighth-order scheme for the high-order fluxes and a donor cell scheme for the low-order fluxes. Photoionization processes are included using the three-group SP_3 model developed by *Bourdon et al*. [2007].

[11] The "two-step" simulation technique proposed by *Qin et al*. [2012a] is used to model the initiation of streamers from sprite-halo events. The technique can be briefly summarized as follows. In the first step, we model the sprite halo dynamics in a simulation domain that extends from the ground up to 95 km, with a radius of 95 km and perfectly conducting boundary conditions using a grid with a spatial resolution of 237.5 m. We keep complete track of the electric field $\vec{E}_{\mathrm{halo}}(r,z,t)$ in the upper atmosphere in this step, and then use this field as an externally applied electric field during the second step to model possible sprite streamer initiation. The simulation domain in the second step extends 2 km vertically and has a radius of 0.25 km with open boundary conditions, and it is discretized in different simulations using grids with at least 3201×401 grid points, corresponding to a spatial resolution of 0.625 m. The variation of air density with altitude is accounted for, and the initial electron and ion densities in the streamer simulation domain are the same as these in the

corresponding region in sprite halo modeling. In order to monitor the possible streamer initiation, we place a Gaussian inhomogeneity (see equation (12)) at different altitudes (e.g., 75.25, 76.25 km in the +CG cases and 75.75, 76.75 km in the -CG cases) on the axis of the halo, and use a streamer model to simulate the evolution of this test inhomogeneity under application of $\overrightarrow{E}_{\text{halo}}(r,z,t)$.

[12] The waveform for lightning current moment is modeled using the formulation proposed by *Cho and Rycroft* [1998]:

$$Ih_Q(t) = \frac{Qh_Q}{12t_0}\left(\frac{t}{t_0}\right)\exp\left[-\left(\frac{t}{t_0}\right)^{1/2}\right] + Ih_{Q0}\ \text{m}^{-3} \qquad (10)$$

where the shape of the return stroke pulse can be controlled by adjusting the charge moment change Qh_Q and the impulsiveness factor t_0, and Ih_{Q0} represents the continuing current moment. A value of t_0=25 μs, which is shown to represent typical +CGs [*Cho and Rycroft*, 1998], is used in the present work, and a smaller t_0 leads to a more impulsive current waveform. Figure 1 shows three representative current waveforms that are used in the present work. We note that for t_0=25μs, the peak density of current moment $Ih_{Q\text{peak}}$ appears at t=4t_0=0.1 ms, and $Ih_Q(t$=40t_0=1 ms) = 0.13$Ih_{Q\text{peak}}$ (i.e., the duration of the lightning current corresponding to t_0=25 μs is ~1.0 ms, see Figure 1 for illustrations of the lightning pulse duration).

[13] The ambient electron density profile can be expressed as [*Wait and Spies*, 1964]:

$$n_e(h) = 1.43\times10^{13}e^{-0.15h'}e^{(\beta-0.15)(h-h')} \qquad (11)$$

where h' [km] and β [km^{-1}] are given parameters describing reference altitude and sharpness, respectively. We assume that h'=85 km and β=0.5 km^{-1}, which represent a typical nighttime electron density profile [e.g., *Han and Cummer*, 2010a]. The positive ion density n_{ion} is assumed to be equal to the electron density at high altitudes, where electron density is higher than 10^8 m^{-3}, and is equal to 10^8 m^{-3} at lower altitudes [e.g., *Narcisi*, 1973]. Initial ambient negative ion density is then calculated based on charge neutrality. We refer to the above density profiles as the "typical nighttime conditions" and use them in most of our simulations in the present work except when specified in subsequent sections.

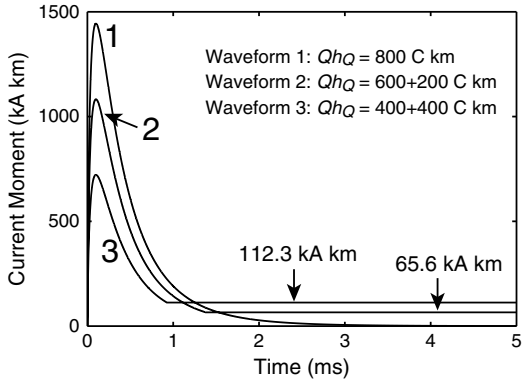

Figure 1. Lightning Current waveform 1: Qh_Q=800 C km and t_0=25 μs; Waveform 2: Qh_Q=600 C km, t_0=25 μs, and continuing current with current moment of Ih_{Q0}=65.6 kA km; Waveform 3: Qh_Q=400 C km, t_0=25 μs and continuing-current with current moment of Ih_{Q0}=112.3 kA km. The total charge moment change over 5 ms is 800 C km for all cases.

[14] The initial inhomogeneities are assumed to be formed by equal amounts of electrons and positive ions (i.e., are charge neutral) that have a spherically symmetric Gaussian density distribution:

$$n_{\text{inhomo}} = n_{\text{peak}}e^{-\frac{r^2}{r_0^2}} \qquad (12)$$

where n_{peak} and r_0 are, respectively, the peak density and the characteristic size of the inhomogeneity. At ground pressure, typical streamer radius and electron density in a streamer channel are, respectively, ~2×10^{-4} m and ~10^{20} m^{-3} [*Pasko et al*., 1998, and references therein]. According to the similarity laws proposed by *Pasko et al*. [1998], these values are, respectively, ~6 m and ~10^{11} m^{-3} at 75 km altitude, or ~13 m and ~2×10^{10} m^{-3} at 80 km altitude. Unless specified in the text, in our simulations, r_0=30 m, which is approximately equal to the size of streamers at ~80 km, and n_{peak}=2×10^9 m^{-3}.

3. Terminology

[15] Before presenting modeling results, it is necessary to clarify the physical concepts of a "sprite halo" and a "streamer initiation region (SIR)" used in the present study.

[16] Originally, the term "sprite halo" was introduced by *Barrington-Leigh et al*. [2001] to refer to the optical emissions of "a brief diffuse flash sometimes observed to accompany or precede more structured sprites in standard-speed video." These authors have also shown that these diffuse optical emissions are produced by the lightning-induced quasi-static electric field interacting with lower ionospheric electrons, rather than the lightning electromagnetic pulse that leads to another type of TLEs named elves [e.g., *Fukunishi et al*., 1996; *Inan et al*., 1997]. In the present work, we use the terms "sprite halo" or simply "halo" to refer to large-scale electrodynamic (i.e., relaxation of the electric field and changes in electron mobility due to electron heating) and chemical (i.e., ionization, attachment and detachment) response of the lower ionosphere to the quasi-static electric field produced by lightning charge removal in the underlying thunderstorm, and use the term "diffuse glow" to define the optical manifestation of this response. We note that in existing literature and in our work, sprites with bright vertical streamer structure are very commonly referred to as simply sprites. We also note that in all sprite halo events modeled in the present study, we always assume that strong electron density inhomogeneities are present in the lower ionosphere, from which sprite streamers are initiated by locally enhanced electric field around these inhomogeneities. Sprite halos and sprite streamers in this context are closely interlinked phenomena as both are driven by quasi-static electric fields produced by lightning. The optical manifestation of these phenomena depends on magnitude and time dynamics of the charge moment change and lower ionospheric conditions (i.e., electron density profile and presence of inhomogeneities). When the diffuse glow of sprite halo is the only visible emission, it does not mean that sprite streamers are not present in the same volume as they usually require additional exponential growth to become visible [e.g., *Liu et al*., 2009]. Similarly, when only sprite streamers are observed optically the diffuse sprite halo emissions may remain subvisual.

[17] A "streamer initiation region" (SIR) refers to a mesospheric/lower ionospheric region in which the reduced lightning-induced electric field E_{halo}/E_k is large enough and persists long enough so that sprite streamers can be initiated from preexisting electron density inhomogeneities in the ambient ionosphere (see Figure 3). This region is relatively small when compared to the entire region where sprite streamers, once initiated, can propagate and develop into a full sprite (see Discussion section). *Qin et al*. [2011] first introduced this concept because preexisting inhomogeneities are randomly located in the ambient ionosphere so that it is impossible to know the exact locations at which sprite streamers will be initiated, and we can only determine a region inside which streamer initiation is possible.

4. Results

4.1. Initiation of Columniform and Carrot Sprites

[18] We first investigate the impact of the impulsive (no continuing current) charge moment changes Qh_Q on the production of columniform and carrot sprites by +CGs under the "typical nighttime conditions" with h'=85 km, β=0.5 km^{-1} and $n_{ion}=10^8$ m^{-3} (see Model section). The current waveforms of the four +CG cases studied in Figure 2 are associated with Qh_Q values of 800, 600, 500, and 400 C km, respectively, and t_0=25 μs in equation (10) (the curve labeled "waveform 1" in Figure 1 corresponds to the case of Qh_Q=800 C km). Note that the duration of the lightning current corresponding to t_0=25 μs is ~1.0 ms (see Figure 1).

[19] In order to divide the upper atmosphere into different streamer initiation regions, we place test inhomogeneities at different mesospheric altitudes and simulate their evolution under the application of lightning-induced electric field $\vec{E}_{halo}(r,z,t)$. Figure 2 shows the subdivisions for a given test inhomogeneity associated with $n_{peak}=2\times10^9$ m^{-3} and r_0=30 m in equation (12). The two-step simulations self-consistently calculate the approximate sprite onset altitudes for given lightning current waveforms, as shown in Figure 2. It is interesting to note that the smallest charge moment change (i.e., 400 C km) in Figure 2 allows the highest possible streamer onset altitude (~81 km with dielectric relaxation time $\tau \simeq 1.5$ ms due to ambient conductivity). Results clearly show that a larger charge moment change leads to lower sprite onset altitudes. This happens because a large charge moment change enhances the conductivity at high altitudes, which is counterproductive for streamer initiation in this region. For +CGs that produce large charge moment changes, such as the cases shown in Figure 2a, b and c, the upper atmosphere can be divided into four sub-SIRs. An important feature in these cases is that Double-SIRs are present, and each is sandwiched by two Single-SIRs. In the parametric study we also found that ~ 320 C km is the minimum charge moment change that is required for a +CG to initiate streamers under typical nighttime conditions.

[20] In our "two-step" simulations corresponding to the parametric study shown in Figure 2, we found that upward negative streamers are only able to initiate in a region where mesospheric electric field $E_{halo}(r,z,t)$ persists with $\gtrsim 0.8\ E_k$

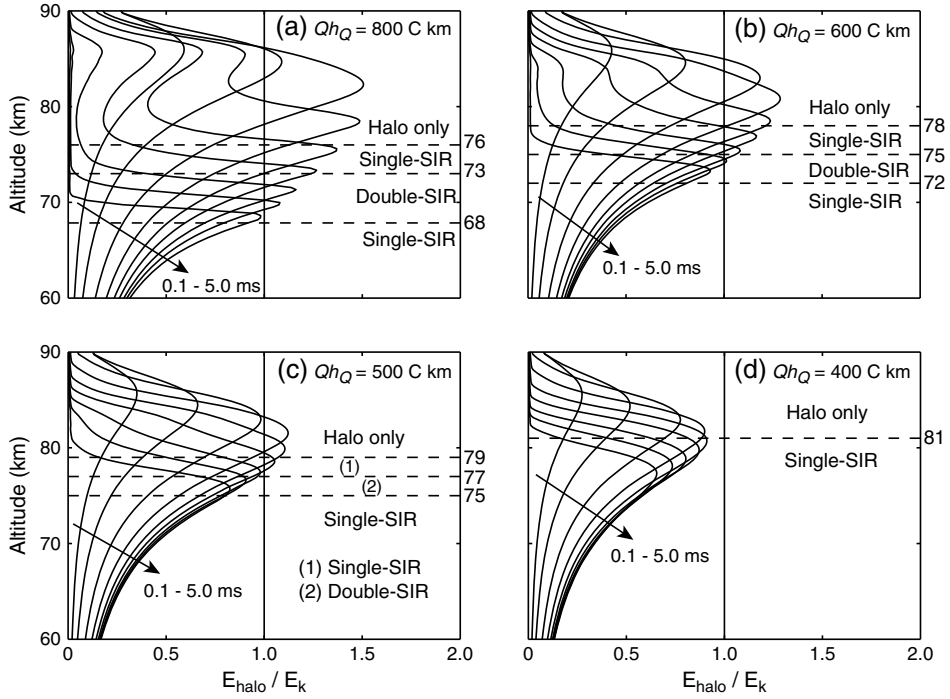

Figure 2. Reduced electric field E_{halo}/E_k along the axis of symmetry of sprite halos at t=0.1, 0.2, 0.4, 0.7, 1.1, 1.6, 2.4, 3.4, 5.0 ms produced by +CGs associated with total charge moment changes of (a) 800 C km (b) 600 C km (c) 500 C km and (d) 400 C km, and division of the upper atmosphere into different sub-SIRs for an inhomogeneity associated with $n_{peak}=2\times10^9$ m^{-3} and r_0=30 m. "Single-SIR" and "Double-SIR" denote single and double-headed streamer initiation region, respectively. Note that the duration of the lightning current corresponding to t_0=25 μs is ~1.0 ms (see Figure 1).

for ≳2 ms, whereas downward positive streamers are able to initiate as long as $E_{halo}(r,z,t)$ persists with ≳ $0.5E_k$ for several milliseconds. This difference leads to two important results shown in Figures 2d and 3, respectively. First, in the case of a +CG with a small charge moment change such as 400 C km, the double-SIR is absent due to the fact that the entire lower ionosphere is under sub-breakdown condition (see Figure 2d), and it is found that ∼500 C km is the minimum charge moment change that can produce carrot sprites under typical nighttime conditions. Second, for large charge moment changes such as 800 C km, it is expected that carrot sprites are able to initiate close to the center of the sprite halo in a region where lightning-induced electric field persists at above $\sim 0.8E_k$ for ≳2 ms, whereas in the same event, columniform sprites may appear at the periphery of the sprite halo where the electric field lasts for only ∼1 ms above $0.8E_k$ or persists at $0.5E_k \lesssim E_{halo} \lesssim 0.8\ E_k$ for several milliseconds (see Figure 3).

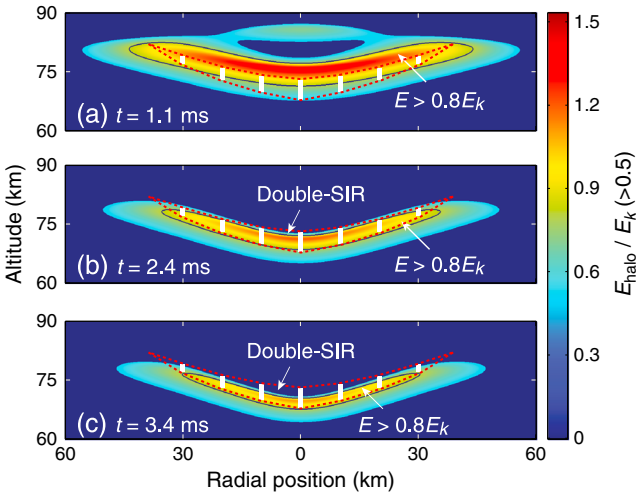

Figure 3. Reduced electric field E_{halo}/E_k (>0.5) of a sprite halo at t=1.1, 2.4, 3.4 ms produced by a +CG associated with Qh_Q=800 C km and t_0=25 μs (i.e., the same case as that shown in Figure 2a). The closed solid curve inside each panel surrounds a region in which $E>0.8E_k$. We calculate the Double-SIRs at the locations with radial distance R=0, 10, 20, and 30 km off the axis of the sprite halo, and show them in each panel using vertical white bars. The entire Double-SIR surrounded by the closed dashed curve in each panel is estimated based on the calculated vertical bars. We note that the entire Double-SIR is approximately the region where the lightning-induced electric field persists at ≳$0.8E_k$ for ≳2 ms, whereas in other regions where the electric field persists at ≳$0.5E_k$, single-headed streamers can initiate if strong inhomogeneities are present. We also note that streamers do not initiate in the region with large lightning-induced electric field (≳$1.4E_k$ in the studied case) where conductivity enhancement is significant due to ionization in the sprite halo (see panel (a)).

4.2. Effects of Impulsiveness of Lightning Current

[21] In order to investigate the impact of impulsiveness of the initial lightning pulse (i.e., the return stroke) on the initiation and morphology of sprites, we conducted another case study in which we kept all the other conditions the same as those used in Figure 2, and modified only the lightning current waveforms to be more impulsive with t_0=10 μs (see equation (10)). Note that the duration of the lightning current corresponding to t_0=10 μs is ∼0.4 ms. Figure 4 shows the mesospheric electric field $E_{halo}(z,t)/E_k$ on the axis of the sprite halo in this case and the corresponding divisions of the upper atmosphere into different sub-SIRs. When compared to the cases studied in Figure 2a and d, it is clear that more impulsive return strokes (i.e, with larger peak current but identical total charge moment change) lead to higher amplitudes of the peak of the lightning-induced electric field, and therefore produce brighter sprite halos. For example, the maximum of the luminosity of the sprite halo presented in Figure 2a is 60 MR at 77.2 km at t=1.0 ms, whereas the maximum of the luminosity in Figure 4a is 180 MR at 78.8 km at t=0.4 ms. Figures 4a and 4b also show that the upper boundaries of the SIRs are located at 74 km and 80 km, which are lower when compared to the boundaries at 76 km in Figure 2a and at 81 km in Figure 2d, respectively. As will be discussed in Section 5.2, this is due to more significant conductivity enhancement in the sprite halo region in the more impulsive cases, which forces sprite streamers to initiate at lower altitudes.

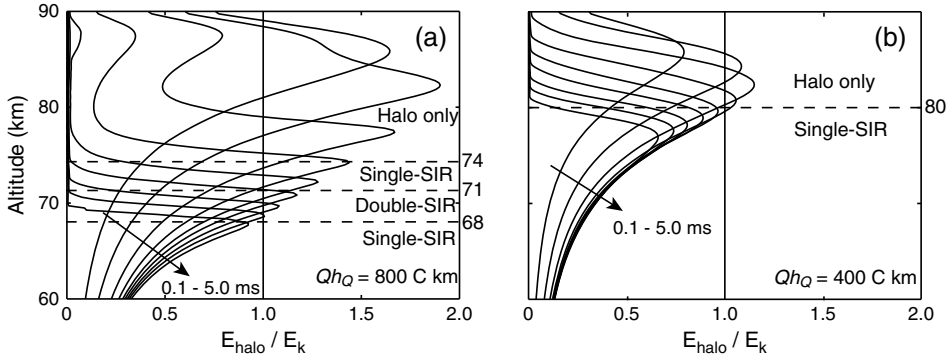

Figure 4. Reduced electric field E_{halo}/E_k along the axis of symmetry of sprite halos at t=0.1, 0.2, 0.4, 0.7, 1.1, 1.6, 2.4, 3.4, 5.0 ms produced by +CGs associated with Qh_Q of (a) 800 C km; (b) 400 C km and t_0=10 μs. Division of the upper atmosphere into different sub-SIRs for an inhomogeneity characterized by $n_{peak}=2\times10^9$ m^{-3} and r_0=30 m. Note that the duration of the lightning current corresponding to t_0=10 μs is ∼0.4 ms.

[22] In Figure 5, we compare the temporal variations of $E_{halo}(t)/E_k$ at three fixed altitudes in different sub-SIRs shown in Figures 2a and 4a to further study the impact of impulsiveness of the initial lightning pulse. We first examine the less impulsive case with Qh_Q=800 C km and t_0=25 μs (dashed lines in Figure 5). According to Figure 2a, the lightning-induced electric field applied at 75 km and at 67 km lead to the production of single-headed downward positive streamers, whereas at 70 km double-headed streamers are able to initiate. If the lightning current is more impulsive with the same total charge moment change and t_0=10 μs (solid lines in Figure 5), according to Figure 4a, the lightning-induced electric field applied at 75 km with strong peak but short persistence only produces halo emissions. We have tested that above 70 km, short persistence of the electric field plays a significant role in impeding upward negative streamer initiation. For example, at 71 km, in the case of less impulsive lightning current, double-headed streamers can be initiated from an inhomogeneity of $n_{peak}=8\times10^8$ m^{-3}, whereas it is still not possible to initiate upward negative streamers with even $n_{peak}=2\times10^9$ m^{-3} in the case of more impulsive lightning current. We note that 70 km is a transition altitude below which the persistence of the electric field in the case of more impulsive lightning is not significantly shorter. At low altitudes such as 67 km, impulsive current is more favorable to initiate single-headed downward positive streamers since the electric field produced by more impulsive lightning is always larger than that of the less impulsive one.

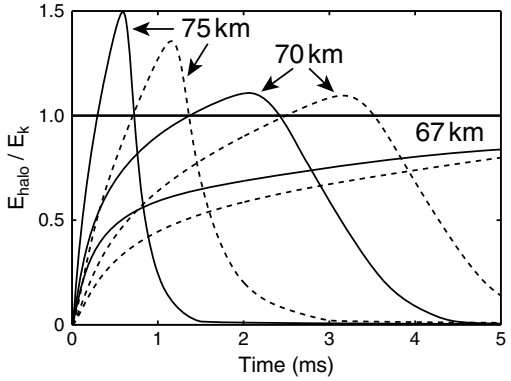

Figure 5. Temporal evolution of the reduced electric field $E_{halo}(t)/E_k$ at 67, 70, 75 km altitudes on the axis of symmetry of sprite halos produced by +CGs associated with Qh_Q=800 C km and t_0=10 μs (solid lines); t_0=25 μs (dashed lines) in equation (10).

[23] We have also conducted similar comparison study for the two cases shown in Figures 2d and 4b in which +CGs produce 400 C km charge moment changes. We note that below ~79 km, that is almost the entire streamer initiation region (see Figures 2d and 4b), the more impulsive lightning produces larger electric field over the 5 ms duration (the comparison is similar to that of 67 km shown in Figure 5), and therefore provides more favorable conditions for the initiation of single-headed downward positive streamers.

4.3. Effects of Continuing Lightning Current

[24] In addition to Qh_Q and t_0 (see equation (10)), continuing current following the initial lightning pulse is another important parameter that may have significant impact on the initiation and propagation of sprite streamers [e.g., *Li et al*., 2008]. Since we only focus on a 5 ms timescale dynamics, in the present work, the "continuing current" can be either the long current tail of a +CG event or continuing current produced by intracloud lightning activities [*van der Velde et al*., 2006]. In the two cases studied in Figure 6, the total charge moment changes are 800 C km. In Figure 6a, the initial lightning pulse produces an impulsive charge moment change of 400 C km, and the continuing current produces another 400 C km (see the curve labeled "waveform 3" in Figure 1). In Figure 6b, the initial pulse and continuing current produce 600 C km and 200 C km charge moment changes, respectively (see "waveform 2" in Figure 1). Unlike the cases shown in Figures 2a and 4a, in which the lightning-induced electric field is effectively screened out above ~70 km at t=5 ms, it is shown in Figures 6a and 6b that the electric field at t=5 ms keeps on a significant strength that is comparable to E_k at up to ~85 km, and the electric field at t=5 ms in Figure 6a is more intense than that in Figure 6b at high altitudes ~80 km.

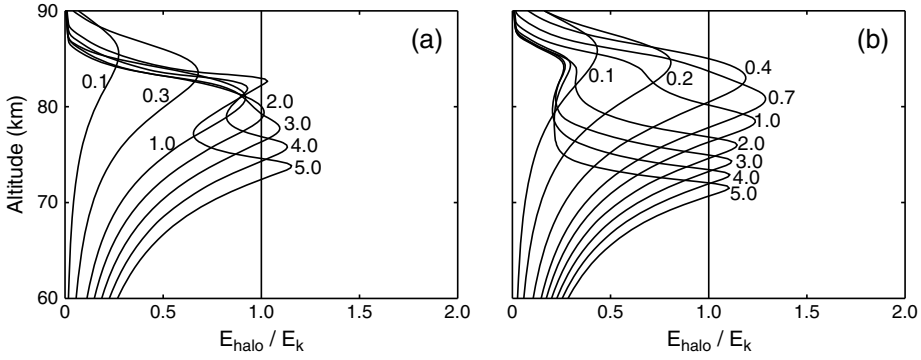

Figure 6. Reduced electric field E_{halo}/E_k on the axis of symmetry of sprite halos in the cases of (a) 400 C km charge moment change produced by the return stroke and additional 400 C km by continuing current associated with a 112.3 kA km current moment; (b) 600 C km charge moment change produced by the return stroke and additional 200 C km by continuing current associated with a 65.6 kA km current moment. We note that the peak halo luminosity integrated over a horizontal line of sight in the case (a) is ~15 MR at 74.6 km at t=5 ms, and in the case (b) is ~15 MR at 72.2 km at t=5 ms.

4.4. Effects of Lightning Polarity

[25] The last lightning property investigated in the present work is the lightning polarity, which according to abundant observations [*Williams et al.*, 2007, 2012, and references therein] most significantly affects the ability of CGs to trigger sprites. Indeed, sprites are almost exclusively produced by +CGs. As will be demonstrated in the present work, this extreme polarity asymmetry stems from the intrinsic differences between positive and negative streamers, and the differences between +CGs and -CGs that were quantitatively emphasized by *Williams et al.* [2012]. For this purpose as well as to predict possible morphological features of the rarely-observed negative sprites, we have used our "two-step technique" to simulate and compare sprite-halo events produced by +CGs and -CGs associated with charge moment changes from 300 to 600 C km under typical nighttime conditions. In this parametric study, we found that for an inhomogeneity with $n_{peak}=2\times10^9$ m^{-3} and $r_0=30$ m, the minimum charge moment change for a +CG to produce positive sprites is ~320 C km, whereas it requires a -CG to produce at least a ~500 C km charge moment change to produce negative sprites. Figure 7 shows the initiation of two double-headed streamers in the mesospheric electric field produced, respectively, by a +CG and a -CG, both associated with Qh_Q=600 C km and t_0=25 μs. We see that in both cases the positive streamer appears at an earlier moment of time than the negative streamer. The dynamics of the streamer initiation in Figure 7 is typical in the case of $Qh_Q \gtrsim$ 500 C km in both +CG and -CG cases.

[26] For a -CG associated with a charge moment change that is smaller than 500 C km, single-headed upward positive streamers may still be able to initiate. However, the dynamics of these streamers is different from the single-headed downward positive streamers produced by +CGs with small charge moment changes. This effect is illustrated in Figure 8 by comparing the luminosities of a single-headed positive streamers initiated by a +CG and a -CG, both associated with Qh_Q=400 C km and t_0=25 μs. As shown in Figure 8, the optical emission of the 1PN$_2$ band system in the downward positive streamer head increases rapidly, whereas the luminosity decreases in the case of upward-propagating positive streamer.

4.5. Effects of Ambient Ionospheric Conditions

[27] Finally, we investigate the impact of the lower ionospheric ambient conditions, that exhibit significant geographical [e.g., *Sagalyn and Burke*, 1985; *Swider*, 1985], short-term [*Han and Cummer*, 2010a, 2010b] and long-term [e.g., *Usoskin et al.*, 2005] variations, on the sprite

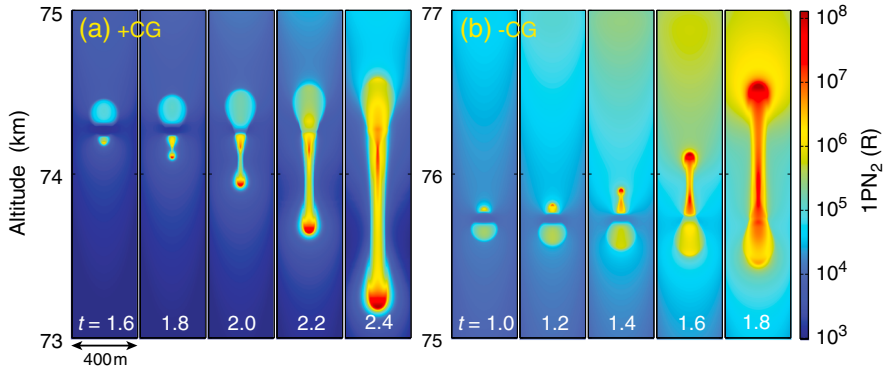

Figure 7. Optical emissions of the 1PN$_2$ band system of a streamer initiated at (a) 74.25 km by a +CG and (b) 75.75 km by a -CG, both associated with Qh_Q=600 C km and t_0=25 μs. We note that the mesospheric electric field $\vec{E}_{\text{halo}}(r,z,t)$ produced by the -CG is almost identical to that produced by the +CG shown in Figure 2b.

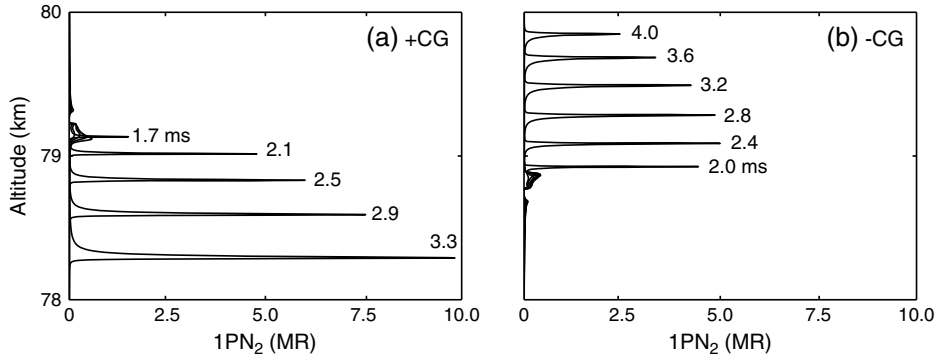

Figure 8. Optical emissions of the 1PN$_2$ band system on the axis of symmetry of a streamer initiated by (a) a +CG and (b) a -CG, both associated with Qh_Q=400 C km and t_0=25 μs (see Figure 2d for the mesospheric electric field $\vec{E}_{\text{halo}}(r,z,t)$ produced by the +CG, which is almost identical to that produced by the -CG.)

morphology. Figure 9 shows a typical case in our parametric study. The +CG is associated with Qh_Q=400 C km and t_0=25 μs, which are the same parameters as those used in Figure 2d. The electron density profile is characterized by h'=87 km and β=0.5 km^{-1}, and the initial ion density is n_{ion}=10^8 m^{-3}. It is shown in Figure 9 that the Double-SIR is very thin in this case. This indicates that for Qh_Q=400 C km, h'=87 km represents the lowest reference altitude that allows production of carrot sprites. Reciprocally, for the upper atmospheric ambient conditions assumed in Figure 9, Qh_Q=400 C km is the minimum charge moment change required for the production of carrot sprites. Figure 10 shows that lower ambient conductivity (i.e., higher h' and smaller n_{ion}) leads to smaller minimum charge moment change required for the production of carrot sprites.

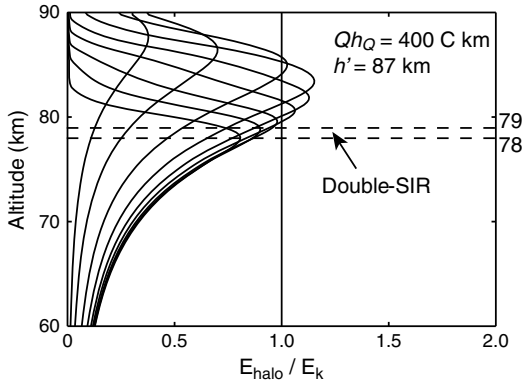

Figure 9. Reduced electric field E_{halo}/E_k along the axis of symmetry of a sprite halo at t=0.1, 0.2, 0.4, 0.7, 1.1, 1.6, 2.4, 3.4, 5.0 ms produced by a +CG associated with Qh_Q=400 C km and t_0=25 μs in equation (10). The electron density profile in this case is defined by h'=87 km and β=0.5 km^{-1} in equation (11). The Double-SIR is calculated for a Gaussian electron inhomogeneity with n_{peak}=2×10^9 m^{-3} and r_0=30 m in equation (12).

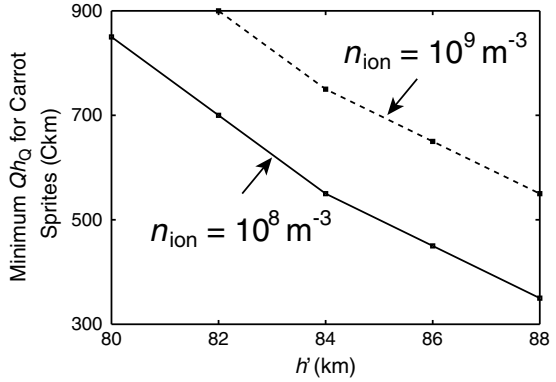

Figure 10. The estimated minimum charge moment changes for the production of carrot sprites under different upper atmospheric ambient conditions that are represented by h' (see equation (11)) and n_{ion}. The quantity n_{ion} is the initial ambient ion density (see Model section). We note that these minimum Qh_Q values are also the threshold for -CGs associated with the same current waveforms to produce sprites, and for the sake of illustration we assume that all the current waveforms have the same parameter t_0=25 μs (see equation (10)) and the test inhomogeneity is characterized by n_{peak}=2×10^9 m^{-3} and r_0=30 m (see equation (12)).

5. Discussion

[28] In the following Subsections 5.1, 5.2, and 5.3, we discuss the impact of several lightning characteristics, including the total charge moment change, the impulsiveness of the initial lightning pulse, and the continuing lightning current on the production of columniform and carrot sprites in the case of +CGs (i.e., positive sprites). In the subsection 5.4, we discuss the threshold charge moment change required for the initiation of 'negative sprites', their possible morphologies, as well as the lightning polarity asymmetry in producing sprites. As already noted above, we assume "typical nighttime conditions," which are defined by an electron density profile characterized by h'=85 km and β=0.5 km^{-1} (see equation (11)), and an initial ion density profile represented by n_{ion}=10^8 m^{-3}. Finally, we discuss the dependence of sprite morphology on the lower ionospheric ambient conditions in the Subsection 5.5.

5.1. Columniform Sprites Are Produced in Sub-Breakdown Conditions

[29] *Kosar et al.* [2012] have reported simulation results on successful formation and stable propagation of positive streamers that initiate from an ionization patch attached to an electrode in sub-breakdown ($E < E_k$) conditions. It was also observed by *Kosar et al.* [2012] that even in an applied electric field that is significantly stronger than the minimum field E_{cr}^- required for their stable propagation, negative streamers fail to start after positive streamers have propagated a long distance [*Kosar et al.*, 2012]. Indeed, our parametric study using "two-step" technique show very stringent requirements for the initiation of negative streamers. It is found that single-headed downward positive streamers, that may develop into columniform sprites, can be initiated either in the upper Single-SIR where the initial large lightning-induced electric field E_{halo} lasts for ≳1 ms above 0.8E_k, or in the lower Single-SIR where E_{halo} persists for several milliseconds at values ≳0.5E_k to ∼0.8E_k (see Figures 2 and 4). In contrast, double-headed streamers or secondary upward negative streamers [*Qin et al.*, 2012a] are initiated in the Double-SIR in which $E_{halo}(t)$ persists at values ≳0.8E_k for ≳2 ms.

[30] With the presence of upper Single-SIR and Double-SIR, +CGs associated with large charge moment changes (>500 C km under typical nighttime conditions) are able to produce carrot sprites if strong inhomogeneities exist in these two regions. As has been indicated by *Qin et al.* [2012a], single-headed downward streamers initiated from inhomogeneities in the upper Single-SIR will favor the development of carrot sprites, since secondary upward negative streamers would be able to initiate in the Double-SIR from previous downward streamer channels. In such cases, single-headed downward positive streamers will appear at higher altitudes at earlier moments of time than upward negative streamers in carrot sprites as observed by *McHarg et al.* [2007] and *Stenbaek-Nielsen and McHarg* [2008]. In the case when strong preexisting inhomogeneities are present in the Double-SIR, double-headed streamers can be initiated and develop into a carrot sprite (see Figure 1 in *McHarg et al.*, 2011). Therefore, it is expected that +CGs

associated with large charge moment changes tend to produce carrot sprites, since the presence of strong inhomogeneities in the lower Single-SIR is likely to be less probable than that in the Double-SIR or in the upper Single-SIR, due to exponential decrease of ambient electron density at lower altitudes.

[31] We conclude that in general, +CGs associated with small charge moment changes ($Qh_Q \lesssim 500$ C km for typical nighttime conditions) are only able to produce columniform sprites. However, we emphasize that not all columniform sprites are produced by +CGs associated with small charge moment changes, since they may also appear at the periphery of a sprite halo induced by a +CG associated with a large Qh_Q (see Figure 3 and observations of *Vadislavsky et al*. [2009, Figure 1a]). As already noted before, streamers initiated in the upper Single-SIR will develop into carrot sprites, therefore, it can be stated that columniform sprites are produced in sub-breakdown conditions (i.e., in the lower Single-SIR or the periphery of a sprite halo produced by a large Qh_Q, or in the entire SIR produced by a small Qh_Q). We note that the range of 320-500 C km charge moment changes that lead to the production of columniform sprites agrees well with observations reported by *Cummer and Inan* [1997]; *Adachi et al*. [2004]; *Hayakawa et al*. [2004]; and *Suzuki et al*. [2011]. This also indicates that the electron density profile characterized by h'=85 km and β=0.5 km^{-1} indeed represents a typical nighttime profile [*Barrington-Leigh et al*., 2001; *Han and Cummer*, 2010a]. We also note that smaller instantaneous charge moment change allows higher streamer initiation altitudes (see Figure 2). This result is consistent with the observations of *Stenbaek-Nielsen et al*. [2010], which show that, statistically, columniform sprite onset altitudes are higher than those of carrot sprites.

[32] We note that although the production of columniform sprites requires smaller charge moment changes when compared to that of carrot sprites, and +CGs associated with small charge moment changes are much more frequent [*Williams et al*., 2007], these do not necessarily lead to the conclusion that columniform sprites occur more frequently. Indeed, in our simulations we have observed that the threshold density of the inhomogeneity required for the initiation of streamers in the case of small Qh_Q is higher than that in the case of large Qh_Q. This is because in the case of small Qh_Q, lightning-induced electric field is small, and therefore a strong inhomogeneity is needed to produce a large space charge field by its polarization in order to produce intense ionization in a local region to initiate streamers.

5.2. Impact of the Impulsiveness of the Initial Lightning Pulse on Streamer Initiation and Sprite Morphology

[33] *Qin et al*. [2011] have concluded that the ability of producing sprites is determined mainly by the total charge moment change of the lightning discharge but not the lightning current duration, whereas the ability of producing detectable halo depends on its impulsive characteristic (see paragraph [45] in Section 5.3). Nevertheless, the lightning impulsive characteristic may still slightly affect the initiation of sprite streamers, and may have great impact on the sprite morphology, which is the subject of the present section.

[34] For the typical nighttime conditions assumed in the present work, streamers are not able to initiate above 81 km due to high ambient conductivity that leads to short relaxation time $\tau \lesssim 1$ ms. The ionization process in the halo region of high ambient electron density only leads to simple collective multiplication of electrons [*Barrington-Leigh et al*., 2001] without strong local space charge effects that are of essential importance to the transition of electron avalanches into sprite streamers [*Qin et al*., 2011]. On the other hand, as already suggested by *Barrington-Leigh et al*. [2001], the ionization process in the sprite halo region increases the conductivity in this region, that will enhance the electric field below, and it therefore may affect the formation of streamers at low altitudes.

[35] In order to better understand the effects of the conductivity enhancement in a sprite halo region, we compare two +CGs associated with the same total charge moment change (Qh_Q=800 C km), but with different impulsiveness (t_0=25 and 10 μs, respectively), in terms of their ability to initiate sprite streamers (see Figure 5). As mentioned in Section 4.2, the +CG associated with a more impulsive initial pulse will produce a brighter halo at high altitudes, since it creates larger mesospheric electric field that also leads to more intense large-scale ionization. These modeling results are consistent with the observational evidence of the relation between the halo luminosity and the lightning impulsiveness documented by *Williams et al*. [2012]. As shown in Figure 5, in the upper part of the SIR $\gtrsim$70 km (such as at 75 km), where the ionization process is dominant for a brief period, although the peak amplitude of the lightning-induced electric field is larger in the case of a more impulsive +CG, the persistence of the electric field is shorter. This is due to a more significant conductivity enhancement by the ionization process at high altitudes in the more impulsive case. Our "two-step" simulations show that above $\sim$70 km, in spite of higher peak amplitude, the shorter persistence of the electric field in the case of a more impulsive +CG leads to the requirement of a stronger inhomogeneities in order to initiate streamers. On the other hand, the situation is different at low altitudes where attachment process dominates ($\lesssim$ 70 km in Figure 5). In this lower part of the SIR, the electric field produced by a more impulsive +CG is always larger, and therefore is more favorable for streamer initiation. The above-discussed effects in the lower and upper part of a streamer initiation region, along with the random location of inhomogeneities, lead to different possible effects of the impulsiveness of a +CG associated with a large charge moment change on the streamer initiation. We expect that in some cases, if strong inhomogeneities are only present at high altitudes, a very impulsive +CG may produce only a bright sprite halo without visible streamer structures, even if the charge moment change is large. In other cases, if inhomogeneities exist at low altitudes, a more impulsive +CG produces a brighter halo at high altitudes, and at the same time has larger probability to initiate streamers at lower altitudes.

[36] Unlike the complicated situations in the case of large charge moment changes, we expect that more impulsive +CG associated with a small charge moment change ($\lesssim$ 500 C km for typical nighttime conditions) has a larger probability to produce sprites, since the electric field strength in almost the entire SIR is higher than that in the case of a less impulsive +CG associated with the same charge moment change (see Section 4.2 for a case study of 400 C km). This may account for the results of *Adachi et al*. [2004] who reported that the number of columns in each columniform sprite event was proportional to the peak current intensity,

which is almost independent of the charge moment change in the sprite-producing +CGs.

[37] Although we conclude that more impulsive +CG has a higher probability to initiate streamers at low altitudes for large charge moment changes, or everywhere for small charge moment changes, we emphasize that in either case, this effect is not as significant as the total charge moment change, since the advantage gained by the impulsiveness, for example in the 400 C km case shown in Figure 4b, can be easily surpassed by an extra ∼20 C km charge moment change in the less impulsive case shown in Figure 2d.

[38] Furthermore, we suggest that the conductivity enhancement at high altitudes has a significant impact on the propagation of the upward negative streamers initiated in the Double-SIR. As discussed in Section 5.1, +CGs associated with large charge moment changes are able to initiate double-headed streamers from ambient inhomogeneities or secondary upward negative streamers from previous downward positive streamers in Double-SIR [*Qin et al*., 2012a]. However, as shown in Figure 2a, the relaxation of the lightning-induced electric field at high altitudes (above ∼70 km) is fast due to the conductivity enhancement, and the electric field decreases to almost zero at high altitudes. This conductivity enhancement not only disables streamer initiation at altitudes 76-81 km, but also impedes the propagation of upward negative streamers that are initiated in the Double-SIR. We note that streamer initiation at 76-81 km is possible in the case of small charge moment change that does not lead to a significant conductivity enhancement (see Figure 2d). In the case of $500 \lesssim Qh_Q \lesssim 600$ C km, the diffuse part of carrot sprites may be faint, as we observe in simulations that the electric field in negative streamer heads are $\lesssim 2E_k$ after a propagation over ∼1 km upward. These streamers apparently do not have much more space to further develop, since lightning-induced electric fields are quickly screened out above the Double-SIR (see Figures 2b, 2c). We suggest that these intermediate charge moment changes with no continuing current account for the "sliding scale from pure columniform sprites to carrot sprites" as discussed by *Stenbaek-Nielsen and McHarg* [2008].

5.3. Continuing Current is of Essential Importance to the Development of the Upper Diffuse Region of Carrot Sprites

[39] Owing to the significant conductivity enhancement, sprite streamers, especially upward negative streamers, are not able to initiate in the halo region with strong lightning-induced electric field (see Figure 2). In particular, this conductivity enhancement, along with the ambient conductivity, effectively screens out the lightning-induced electric field at high altitudes. The stable propagation of negative streamers requires a minimum applied electric field $E_{cr}^{-} \simeq 12.5\mathrm{N/N_0}$ kV/cm [*Pasko et al*., 2000], or even $\gtrsim 15\mathrm{N/N_0}$ kV/cm [*Celestin and Pasko*, 2010]. Thus, the fast relaxation of the lightning-induced electric field above the Double-SIR leads to a fast decay and eventually termination of the upward propagating negative streamers. This explains the observations which show that the upper diffuse part of carrot sprites usually terminates inside the bright sprite halos that lead to significant conductivity enhancement (see Figure 2a in *Taylor et al*. [2008] and Figure 1 in *Pasko et al*. [2011]).

[40] From the discussion in Section 5.2, we can expect that +CGs associated with weak initial pulses but accompanied by intense continuing current may provide favorable conditions for the initiation and propagation of upward negative streamers, since these +CGs do not significantly enhance the conductivity at high altitudes (i.e., the sprite halo is dim or sub-visible) and therefore allow longer persistence of the lightning-induced electric field. This is demonstrated in Figure 6. Although the +CG event modeled in Figure 6a produces the same total charge moment change of 800 C km as that in Figures 2a and 4a, it produces less ionization, which leads to a dimmer halo (see caption of Figure 6) and slower relaxation at high altitudes (∼80 km). Meanwhile, the intense continuing current compensates the loss of the electric field due to dielectric relaxation, and therefore the electric field below ∼85 km can persist at a level that is comparable to E_k. We note that the double-peaked structure of the electric field at t=5 ms in Figure 6a corresponds to structure of conductivity modification at different altitudes. The electron density enhancement at ∼75 km is more significant than that at ∼82 km and ∼72 km, which leads to faster electric field relaxation at ∼75 km. When compared to the case shown in Figure 6a, stronger electric field produced by the initial lightning pulse in Figure 6b enhances the conductivity at high altitudes (∼80 km) more significantly, and with a less intense continuing current, the electric field at high altitudes persists at a much lower value ($\sim 0.25E_k$).

[41] Besides, when comparing the two cases shown in Figures 2d and 6a, or the ones shown in Figures 2b and 6b, in which the initial lightning pulse is or is not followed by continuing lightning current, it is apparent that continuing lightning current significantly enhances the mesospheric electric field at low altitudes after the completion of the initial lightning pulse. It is reasonable to expect that continuing lightning current with tens to hundreds of millisecond durations has similar effects on the mesospheric electric field, and therefore is one critical reason that leads to the production of the so-called long-delayed sprites, as emphasized by *Li et al*. [2008].

[42] The above simulation results are consistent with the observations of *van der Velde et al*. [2006] and *Suzuki et al*. [2011] in which carrot sprites are produced by larger total charge moment changes in the lightning events with intense continuing current, whereas columniform sprites are produced by instantaneous charge moment changes during +CG events with transient current.

5.4. Negative Sprites Should be Necessarily Carrot Sprites Produced by -CGs Associated With Large Charge Moment Changes

[43] We first note that the mesospheric electric fields $\vec{E}_{\mathrm{halo}}(r,z,t)$ produced by the -CGs studied in the present work are not shown in separate figures since they are almost identical to those shown in Figure 2 produced by the +CGs associated with the same current waveforms (see also discussions of *Qin et al*. [2011, Section 5.1] on the "Polarity Symmetry of +CGs and -CGs in Producing Sprite Halos"). It should be therefore emphasized that the results shown in Figures 2 through 6 can also be used for the discussion of -CG cases or comparison between +CGs and -CGs as the resulting electric fields in the halo region would be very similar on the considered timescale. For example, assuming that

the results shown in Figure 2 are related to -CGs, under typical nighttime conditions, a minimum Qh_Q of ∼500 C km (see panel (c) of Figure 2) is required for the production of 'negative sprites', since otherwise downward negative streamers cannot be initiated. In the same vein, one can also think the results shown in Figure 4 (i.e., the more impulsive cases) as related to -CGs and study the impact of the difference between the impulsive characteristics of +CGs and -CGs by comparing these results with those shown in Figure 2.

[44] In all of our "two-step" simulations of sprite streamers produced by either +CGs or -CGs, initiation of positive streamers is always easier and earlier than that of, if even present, negative streamers from the same initial electron inhomogeneities. Therefore, the positive sprites can be in the form of either columniform sprites with only downward positive streamers or carrot sprites with both upward negative and downward positive streamers. However, from the study carried out in the present paper we conjecture that negative sprites are likely always carrot sprites, and are unlikely to be upward propagating columniform sprites. The main reason is that in the case of small charge moment changes, the single-headed upward positive streamers produced by -CGs, that potentially can lead to columniform shapes, do not have a ∼5-10 km region [*Wescott et al*., 1998] with sufficient electric field to develop because of the fast electric field relaxation at high altitudes. The lack of concomitant large peak current and intense continuing current in -CG events [*Saba et al*., 2006; *Saba et al*., 2010; *Williams et al*., 2012] prevents long persistence of the lightning-induced electric field at high altitudes similar to that produced by +CGs with intense continuing current (see Figure 6). In contrast to the fast growing luminosity in the single-headed downward positive streamer produced by a +CG (see Figure 8a), the luminosity in the single-headed upward positive streamer head produced by a -CG decreases quickly (see Figure 8b). These decaying single-headed upward positive streamers could potentially be detected as bright spots/patches, but not as 5-10 km columns. Interestingly, it seems that this kind of bright spots/patches exist in previous 'negative' sprite observations (see the bright spot at the right side of the sprite halo documented in *Taylor et al*. [2008, Figure 2]). We conjecture that they may also appear in some possibly sub-visible sprite halos produced by -CGs associated with intermediate large charge moment changes (e.g., 400 C km), but were not previously considered as sprite streamers or may be too dim to be detected.

[45] Nevertheless, when thinking of sprites as objects with extensive vertical structures (i.e., longer than ∼5 km, which is the shortest length of typical columniform sprites (e.g., *Wescott et al*. [1998]), 'negative' sprites are most likely carrot sprites. In the sense that downward negative streamers must be initiated in order to develop extensive vertical structures, we calculate that a minimum charge moment change of ∼500 C km is required for a -CG to produce sprites under typical nighttime conditions. This value is expected, since it should be close to that required for the production of carrot sprites in the case of +CGs. We note that the charge moment changes producing the 'negative' sprites documented by *Barrington-Leigh et al*. [1999] (1550 and 1380 C km) and *Taylor et al*. [2008] (503 C km in the first 2 ms) are all above this threshold. *Li and Cummer* [2011] recently reported observations of 6 'negative sprite' events, in which the charge moment charges of the causal -CGs are all larger than 450 C km and up to ∼1000 C km.

[46] The larger threshold charge moment change (∼500 C km in the case of a -CG compared to ∼320 C km in the case of a +CG under typical nighttime conditions) required for the initiation of downward negative streamers partially accounts for the rarity of negative sprites when compared to occurrence of positive sprites. Moreover, we emphasize that in our "two-step" simulations, we can only model the very early stage of sprite streamer development (i.e., the inception stage). These streamers have to undergo significant acceleration and expansion before they become observable [*Liu et al*., 2009; *Qin et al*., 2012a]. It is also known that the minimum applied electric field required for the stable propagation of negative streamers ($E_{cr}^{-} \simeq 12.5$ kV/cm at ground level) is higher than that required for the stable propagation of positive streamers ($E_{cr}^{+} \simeq 4.4$ kV/cm at ground level) [*Pasko et al*., 2000]. These two effects lead to a larger difference of threshold charge moment changes required for +CGs and -CGs to produce observable sprites in comparison with the difference between 500 C km and 320 C km. The above-discussed different threshold charge moment changes required for streamer initiation and different applied electric field required for stable propagation growth of positive and negative streamers [*Pasko et al*., 2000] represent two critical reasons for the polarity asymmetry of +CGs and -CGs in the production of sprites. These two reasons stem from the essential differences between positive and negative streamers, and therefore even if +CGs and -CGs had no intrinsic differences, +CGs would still more easily produce sprites.

[47] In fact, +CGs and -CGs are intrinsically different, as was emphasized quantitatively by *Williams et al*. [2012]. -CGs are usually more impulsive than +CGs, but they do not carry long continuing lightning current as +CGs do [e.g., *Williams et al*., 2012], and the associated charge moment changes are relatively small [e.g., *Williams et al*., 2007; *Lu et al*., 2012]. Intense continuing current in +CG cases facilitates the initiation of long-delayed sprites by removing additional thundercloud charge [*Li et al*., 2008]. On the other hand, we emphasize that the impact of lightning impulsiveness discussed in Section 5.2 for +CG cases is also applicable to the case of -CGs. Since -CGs usually produce small charge moment changes, more impulsive initial lightning pulse is favorable for streamer initiation (see the discussions in Section 5.2). Nevertheless, as stated in Section 5.2, charge moment change plays a much more important role than the impulsiveness in producing sprites. The fact that +CGs produce large charge moment changes much more frequently [e.g., *Cummer and Lyons*, 2005; *Williams et al*., 2007] is another critical reason for the lightning polarity asymmetry in the production of sprites. We note that their more impulsive characteristic is the reason why -CGs, although usually associated with smaller charge moment changes, produce statistically more halos than +CGs do [*Newsome and Inan*, 2010; *Williams et al*., 2012, Section 4], since the peak lightning current is the key parameterin determining the halo luminosity as shown in the present study.

[48] It is important to put the results of the present study in the context of a sprite polarity paradox discussed recently by [*Williams et al*., 2012]. The essence of the paradox is that a

global survey of charge moment changes associated with -CGs indicate that there is a small, but non-negligible number of -CGs that have magnitudes of charge moment changes as large as those that are known to produce sprite discharges in case of +CGs. *Williams et al*. [2012] estimated that the number of -CGs possessing these properties is approximately 10% of the related +CG population worldwide. The paradox is that sprites produced by -CGs are extremely rare (much less that 10% mentioned above), with very few events observed over many years of ground and satellite based observations worldwide [*Williams et al*., 2012, and references therein]. As already acknowledged earlier in our paper, *Williams et al*. [2012] pointed to a significant number of observed halos produced by -CGs and emphasized the importance of more impulsive lightning currents in -CGs in facilitating this phenomenology. The results obtained in our present and previous studies [*Qin et al*., 2011, 2012a] indicate that the significant asymmetry in development of sprite streamers in case of +CGs and -CGs may be the most important factor for understanding why sprites produced by -CGs are so rare. A simple estimate based on the charge moment change data documented by *Williams et al*. [2007] and the charge moment thresholds for initiation of positive and negative sprites obtained in the present study (respectively 320 C km and 500 C km under typical nighttime conditions) has been made by *Qin et al*. [2012b]. This leads to the theoretical result that ~5% of sprites should be negative. However, [*Qin et al*., 2012b] noted that due to a factor of 3 difference in fields required for propagation/growth of streamers of different polarity (see discussion above in this section about the E_{cr}^{+} and E_{cr}^{-} fields) and the resultant intrinsic dimness of negative streamers propagating in a given field as compared to positive streamers, this estimate must be considered as an upper limit for observations. It should be emphasized that initiation of streamers in sprites does not guarantee that streamers are bright enough to be detectable. Indeed, after initiation, streamers in sprites go through a significant exponential growth, when their brightness increases by several orders of magnitude, before they become observable [*Liu et al*., 2009; *Qin et al*., 2012a].

5.5. Dependence of Sprite Morphology on the Upper Atmospheric Ambient Conditions

[49] The upper atmospheric ambient electron density profile plays an essential role in the production of sprite streamers [*Qin et al*., 2011]. Indeed, whether a charge moment change is "large" or "small," in terms of its ability to produce sprite streamers, must be evaluated for a given ambient conductivity profile, because lower ambient electron density leads to a lower threshold charge moment change required for the production of sprite streamers [*Qin et al*., 2011]. In the present work, we found a similar dependence of the threshold charge moment change required for the production of carrot sprites in +CG cases on the lower ionospheric conductivity profile (see Figure 10 and a typical case in Figure 9). Namely, lower ambient conductivity (i.e., larger h' and smaller n_{ion}) leads to smaller threshold charge moment changes required for the production of carrot sprites by +CGs. We note that these minimum charge moment changes also represent the threshold for -CGs to produce negative sprites. As discussed in Section 5.4, positive sprites have both columniform and carrot shapes, but as far as we can envision from the present study negative sprites only have carrot shapes. The minimum charge moment change required for the production of negative (carrot) sprites is the same as that required for the production of positive carrot sprites (due to polarity symmetry of halos), which is larger than that required for the production of positive columniform sprites.

[50] The sharpness β of the ambient electron density profile is fixed in the present study in order to limit the number of variables in the parametric study. A sharper β would lead to the increase/decrease of the ambient electron density above/below the altitude h' (see equation (11)), therefore is unfavorable/favorable for production of carrot sprites at higher/lower altitudes.

[51] In the present study, a fundamental assumption is based on the presence of electron density inhomogeneities in the lower ionosphere, from which sprite streamers can be initiated. If one assumes that the ambient densities of electrons and ions are perfectly continuous and varying smoothly on spatial scales of sprite halos, that is no inhomogeneities are present, the response of the ionosphere to a lightning-induced electric field should be large-scale and continuous as no explicit small-scale length exists in this system [*Qin et al*., 2011]. Note that this is fundamentally different from the theory of *Luque and Ebert* [2009], in which a sprite streamer was initiated as an instability in the halo front region where electron density gradients were extremely high. Experimentally, it is a known fact that some +CGs with very large charge moment changes do not produce sprites, and recent studies indicate that the charge moment change is not a perfect indicator of sprites production and should be considered as a necessary but not sufficient condition for sprites [*Lang et al*., 2011]. The absence of inhomogeneities would facilitate this phenomenology. The origin of these lower ionospheric inhomogeneities, however, is still an open question. Recently, *Kosar et al*. [2012] briefly summarized the possible mechanisms that might be attributed to the creation of these inhomogeneities, including ionospheric disturbances created by meteor trails, electrodynamic effects from thunderstorm and lightning, or gravity wave breaking.

[52] In order to make the parametric study more tractable, the exact divisions into different sub-SIRs in Figures 2 and 4 are only obtained for a given spherical inhomogeneity characterized by $n_{peak}=2\times10^{9}$ m^{-3} and $r_0=30$ m in equation (12). A value 2×10^{9} m^{-3} is ~2 orders of magnitude higher than the ambient electron density at sprite altitudes (~80 km), and this value is ~1 order of magnitude lower than the electron density in a streamer channel at ~80 km. This inhomogeneity with $n_{peak}=2\times10^{9}$ m^{-3} is strong enough so that streamers can directly initiate from it (see Figure 7), and stronger inhomogeneities (i.e., higher n_{peak} and larger r_0) will initiate streamers even more favorably. For example, if $n_{peak}=2\times10^{10}$ m^{-3}, under "typical nighttime conditions", the minimum charge moment change required for +CGs to produce columniform/carrot sprites is ~300/450 C km. However, an even higher n_{peak} would not significantly affect the minimum charge moment changes since a value of 2×10^{10} is already as high as the electron density in a streamer channel at ~80 km altitude. In the present study, it is not possible to conduct a study of the minimum charge moment changes associated with inhomogeneity with $n_{peak}=2\times10^{8}$ m^{-3} because this inhomogeneity needs to propagate along the lightning-induced electric field to first develop

as an electron avalanche before turning into a streamer. This process requires a timescale longer than 5 ms and probably a simulation domain larger than 2×0.25 km^2. We further note that the shape of inhomogeneity, such as an elongated ionization patch used by *Kosar et al*. [2012], or elliptically Gaussian distributed inhomogeneity, also plays a role in streamer initiation and therefore affects the subdivisions of SIRs.

[53] Given the importance of the upper atmospheric conductivity profile in sprite streamer initiation and sprite morphology, we summarize several parameters or processes that may partially account for the variation of sprite production in different observation campaigns. First, the geographical variation of conductivity profile may affect the global distribution and occurrence rates of sprites, as the electron density, ion concentration and ion composition at different locations vary significantly [e.g., *Sagalyn and Burke*, 1985; *Swider*, 1985]. Second, significant short-term temporal variability of the nighttime D-region of the ionosphere is well known [e.g., *Han and Cummer*, 2010a, 2010b]. *Han and Cummer* [2010a] probed the ionospheric D-region by measuring the high-power broadband very low frequency signals generated by lightning and propagating in the Earth-ionosphere waveguide in July and August of 2005, and found that the measured nighttime D-region electron density profile heights (i.e., h' in equation (11)) showed large temporal variations of several kilometers on some nights and relatively stable behaviors on others. The measured hourly average nighttime heights in 260 h ranged between h'=82.0 and 87.2 km, with a mean value of 84.9 km [*Han and Cummer*, 2010a], whereas during daytime the h' value can be as low as ~70 km [*Han and Cummer*, 2010b]. Variation of the D-region electron density profile over a range consistent with these ionospheric observations leads to variation of the threshold charge moment change for the production of carrot sprites (see Figure 10) varying by nearly a factor-of-two. Besides, rocket measurements in the D-region of the ionosphere show ion density between 75 and 85 km of about 10^9 m^{-3} near midday, about 10^8 m^{-3} near midnight, with a decay from about 4×10^8 to 10^8 m^{-3} through sunset and a threefold increase at sunrise [*Narcisi*, 1973]. This short-term ion conductivity variation in the lower ionosphere also affects the production of sprites, as shown in Figure 10 that the increase of ambiention density from 10^8 m^{-3} to 10^9 m^{-3} leads to a ~200 C km larger charge moment change required for the production of carrot sprites. Finally, the variation of conductivity in the upper atmosphere due to long-term effects may account for the differences of sprite production observed in different years, for example, due to variation in the solar activity and galactic cosmic ray flux [e.g., *Usoskin et al*., 2005]. We emphasize that besides the above-discussed variations in the ambient conditions of the lower ionosphere, the seasonal variations of the thunderstorm activity in the troposphere [e.g., *Sato et al*., 2008], that lead to different lightning characteristics, will also significantly affect sprite morphologies in different campaigns.

6. Conclusions

[54] A two-dimensional plasma fluid model applied in a "two-step" technique, in which we couple the large-scale halo dynamics and development of small-scale streamers [*Qin et al*., 2012a], is used in the present work to simulate sprite-halo events over a time scale of 5 ms in order to study the dependence of sprite morphology on lightning characteristics and lower ionospheric ambient conditions. The most significant associative detachment process $O^-+N_2 \rightarrow e+N_2O$ in sprite chemistry has been taken into account. The test inhomogeneity from which the streamer is generated has a Gaussian distribution with $n_{peak}=2\times10^9$ m^{-3} and r_0=30 m (see equation (12)). The principal results of the present work are summarized as follows:

[55] 1. Morphology of 'positive' sprites is mainly determined by the total charge moment change of the causative +CGs and the location of initial imhomogeneities. +CGs associated with large charge moment change (Qh_Q) tend to produce carrot sprites, whereas those with small Qh_Q are only able to produce columniform sprites. We have shown that the initiation of the upward negative streamers that form the upper diffuse region of carrot sprites requires the presence of a double-headed streamer initiation region (Double-SIR) in which the lightning-induced electric field persists above $\sim0.8E_k$ for $\gtrsim$2 ms in the upper atmosphere, whereas the initiation of single-headed downward positive streamers that may develop into columniform sprites only requires that the lightning-induced electric field persists at above $\sim0.5E_k$. For typical nighttime conditions (i.e., electron density profile is characterized by h'=85 km, β=0.5 km^{-1} in equation (11), and $n_{ion}=10^8$ m^{-3}, see Section 2), the minimum Qh_Q required for +CGs to produce columniform and carrot sprites are 320 C km and 500 C km, respectively.

[56] 2. Conductivity enhancement inside a sprite halo where ionization processes are dominant for a brief period, on one hand, leads to faster relaxation of the lightning-induced electric field and therefore lowers the probability of streamer initiation at these high altitudes, but on the other hand, enhances the electric field at lower altitudes where attachment processes are dominant and therefore is favorable for streamer initiation in the region below the sprite halo. These different effects inside and below the sprite halo region will be more significant in the case of a more impulsive initial lightning pulse for a given total charge moment change. In the case of small charge moment changes (e.g., $\lesssim$500 C km in typical nighttime conditions) in which only sub-breakdown conditions ($E<E_k$) are produced in the upper atmosphere, a more impulsive initial lightning pulse is more favorable for streamer initiation, since the lightning-induced electric field in almost the whole streamer initiation region will be enhanced.

[57] 3. Conductivity enhancement inside a sprite halo also impedes the development of upward negative streamers and therefore leads to a quick decay and termination of the upper diffuse region of carrot sprites. In the case of a weak initial lightning pulse accompanied by intense continuing current, conductivity enhancement due to ionization inside the halo is less significant (i.e., a dim halo). In such a case, slow dielectric relaxation and continuing current leads to the persistence of large electric field ($\sim E_k$) at high altitudes far above the sprite halo. An extensive upper diffuse region of carrot sprites can therefore develop.

[58] 4. 'Negative' sprites are most likely to be carrot sprites in the sense that upward positive streamers are easier to initiate than downward negative streamers in the case of -CGs. In typical nighttime conditions, a minimum charge moment change of ~500 C km, which is the same as that

required for the production of carrot sprites in the case of +CGs, is required for -CGs to produce sprites. -CGs associated with smaller charge moment changes may still be able to initiate single-headed upward positive streamers. However, these upward streamers cannot develop in a 5-10 km region with sufficient electric field to further develop into columnar shape because of the quick relaxation of electric field above the streamer initiation region, and therefore may only potentially be able to be observed as bright spots/patches.

[59] 5. The different minimum charge moment changes required for streamer initiation found in this paper (320 and 500 C km, respectively, for +CGs and -CGs under typical nighttime conditions), the different applied electric field required for stable propagation of positive and negative streamers [*Pasko et al*., 2000], along with the fact that +CGs much more frequently produce large charge moment changes [e.g., *Cummer and Lyons*, 2005; *Williams et al*., 2007; *Lu et al*., 2012], represent three critical factors for the polarity asymmetry of +CGs and -CGs in the production of sprites. The first two factors stem from the intrinsic differences between positive and negative streamers, and the third one stems from the intrinsic differences between +CGs and -CGs.

[60] 6. The variations of upper atmospheric ambient conditions have a significant effect on sprite production. Lower ambient conductivity (i.e., larger h' and smaller n_{ion}) leads to smaller changes in threshold charge moment required for the production of carrot sprites. We also suggest that these variations can be the geographical [*Sagalyn and Burke*, 1985; *Swider*, 1985], short-term [e.g., *Han and Cummer*, 2010a; *Han and Cummer*, 2010b], and long-term [e.g., *Usoskin et al*., 2005] variations of the upper atmospheric conductivity, which, along with the seasonal variations of thunderstorm activity that lead to different lightning characteristics in the troposphere [e.g., *Sato et al*., 2008], may account for the differences of sprite morphologies observed by *Stenbaek-Nielsen et al*. [2010] in different campaigns.

[61] **Acknowledgments.** This research was supported by the NSF grant AGS-0734083 and DARPA NIMBUS grant HR0011-101-0059/10-DARPA-1092 to the Pennsylvania State University. The authors acknowledge the Research Computing and Cyberinfrastructure unit of Information Technology Services at The Pennsylvania State University for providing HPC resources and services that have contributed to the research results reported in this paper. URL: http://rcc.its.psu.edu.

References

Adachi, T., H. Fukunishi, Y. Takahashi, and M. Sato (2004), Roles of the EMP and QE field in the generation of columniform sprites, *Geophys. Res. Lett.*, *31*(4), L04107, doi:10.1029/2003GL019081.

Barrington-Leigh, C. P.,U. S. Inan, and M. Stanley (2001), Identification of sprites and elves with intensified video and broadband array photometry, *J. Geophys. Res.*, *106*(A2), 1741–1750, doi:10.1029/2000JA000073.

Barrington-Leigh, C. P., U. S. Inan, M. Stanley, and S. A. Cummer (1999), Sprites triggered by negative lightning discharges, *Geophys. Res. Lett.*, *26*(24), 3605–3608.

Bourdon, A.., V. P. Pasko, N. Y. Liu, S. Celestin, P. Segur, and E. Marode (2007), Efficient models for photoionization produced by non-thermal gas discharges in air based on radiative transfer and the Helmholtz equations, *Plasma Sources Sci. Technol.*, *16*, 656–678.

Celestin, S., and V. P. Pasko (2010), Effects of spatial non-uniformity of streamer discharges on spectroscopic diagnostics of peak electric fields in transient luminous events, *Geophys. Res. Lett.*, *37*, L07804, doi:10.1029/2010GL042675.

Cho, M., and M. J. Rycroft (1998), Computer simulation of the electric field structure and optical emission from cloud-top to the ionosphere, *J. Atmos. Solar Terr. Phys.*, *60*, 871–888.

Cummer, S. A., and U. S. Inan (1997), Measurement of charge transfer in sprite-producing lightning using elf radio atmospherics, *Geophys. Res. Lett.*, *24*, 1731–1734, doi:10.1029/97GL51791.

Cummer, S. A., and W. A. Lyons (2005), Implication of lightning charge moment changes for sprite initiation, *J. Geophys. Res.*, *110*, A04304, doi:10.1029/2004JA010812.

Cummer, S. A., N. C. Jaugey, J. B. Li, W. A. Lyons, T. E. Nelson, and E. A. Gerken (2006), Submillisecond imaging of sprite development and structure, *Geophys. Res. Lett.*, *33*, L04104, doi:10.1029/2005GL024969.

Davies, D. K. (1983), Measurements of swarm parameters in dry air, in Theoretical Notes, Note 346, edited by Westinghouse R&D Center, Westinghouse R&D Center, Pittsburgh, PA.

Fukunishi, H., Y. Takahashi, M. Kubota, K. Sakanoi, U. S. Inan, and W. A. Lyons (1996), Elves: Lightning-induced transient luminous events in the lower ionosphere, *Geophys. Res. Lett.*, *23*(16), 2157–2160.

Gerken, E. A., U. S. Inan, and C. P. Barrington-Leigh (2000), Telescopic imaging of sprites, *Geophys. Res. Lett.*, *27*, 2637–2640.

Gordillo-Vazquez, F. J. (2008), Air plasma kinetics under the influence of sprites, *J. Phys. D: Appl. Phys.*, *41*(23), 234016.

Han, F., and S. A. Cummer (2010a), Midlatitude nighttime D region ionosphere variability on hourly to monthly time scales, *J. Geophys. Res.*, *115*, A09323, doi:10.1029/2010JA015437.

Han, F., and S. A. Cummer (2010b), Midlatitude daytime D region ionosphere variations measured from radio atmospherics, *J. Geophys. Res.*, *115*, A10314, doi:10.1029/2010JA015715.

Hayakawa, M., T. Nakamura, Y. Hobara, and E. Williams (2004), Observation of sprites over the Sea of Japan and conditions for lightning-induced sprites in winter, *J. Geophys. Res.*, *109*, A01312, doi:10.1029/2003JA009905.

Inan, U. S., C. Barrington-Leigh, S. Hansen, V. S. Glukhov, T. F. Bell, and R. Rairden (1997), Rapid lateral expansion of optical luminosity in lightning-induced ionospheric flashes referred to as 'elves', *Geophys. Res. Lett.*, *24*(5), 583–586.

Kosar, B. C., N. Liu, and H. K. Rassoul (2012), Luminosity and propagation characteristics of sprite streamers initiated from small ionospheric disturbances at sub-breakdown conditions, *J. Geophys. Res.*, *117*, A08328, doi:10.1029/2012JA017632.

Lang, T. J., J. Li, W. A. Lyons, S. A. Cummer, S. A. Rutledge, and D. R. MacGorman (2011), Transient luminous events above two mesoscale convective systems: Charge moment change analysis, *J. Geophys. Res.*, *116*, 1–2.

Li, J., and S. A. Cummer (2011), Charge moment change and lightning-driven electric field associated with negative sprites, Abstract AE23A-02 presented at 2011 Fall Meeting, AGU, San Francisco, Calif., 5-9 Dec.

Li, J., S. A. Cummer, W. A. Lyons, and T. E. Nelson (2008), Coordinated analysis of delayed sprites with high-speed images and remote electromagnetic fields, *J. Geophys. Res.*, *113*(D20), D20206.

Liu, N. Y. (2012), Multiple ion species fluid modeling of sprite halos and the role of electron detachment of O^- in their dynamics, *J. Geophys. Res.*, *117*, A03308, doi:10.1029/2011JA017062.

Liu, N. Y., V. P. Pasko, K. Adams, H. C. Stenbaek-Nielsen, and M. G. McHarg (2009), Comparison of acceleration, expansion, and brightness of sprite streamers obtained from modeling and high-speed video observations, *J. Geophys. Res.*, *114*, A00E03.

Lu, G., S. A. Cummer, R. J. Blakeslee, S. Weiss, and W. H. Beasley (2012), Lightning morphology and impulse charge moment change of high peak current negative strokes, *J. Geophys. Res.*, *117*, D04212, doi:10.1029/2011JD016890.

Luque, A., and U. Ebert (2009), Emergence of sprite streamers from screening-ionization waves in the lower ionosphere, *Nat. Geosci.*, *2*(11), 757–760, doi:10.1038/NGEO662.

Luque, A., and F. J. Gordillo-Vazquez (2012), Mesospheric electric breakdown and delayed sprite ignition caused by electron detachment, *Nat. Geosci.*, *5*(1), 22–25, doi:10.1038/NGEO1314.

Lyons, W. A. (1996), Sprite observations above the U.S. high plains in relation to their parent thunderstorm systems, *J. Geophys. Res.*, *101*, 29,641–29,652.

Marshall, R. A., and U. S. Inan (2006), High-speed measurements of small-scale features in sprites: Sizes and lifetimes, *Radio Sci.*, *41*, RS6S43, doi:10.1029/2005RS003353.

McHarg, M. G., H. C. Stenbaek-Nielsen, and T. Kanmae (2007), Streamer development in sprites, *Geophys. Res. Lett.*, *34*, L06804, doi:10.1029/2006GL027854.

McHarg, M. G., H. C. Stenbaek-Nielsen, T. Kanmae, and R. K. Haaland (2011), High-Speed Imaging of Sprite Streamers, *IEEE Trans. Plasma Sci.*, *39* (11, Part 1, SI), 2266–2267, doi:10.1109/TPS.2011.2165299.

Morrow, R., and J. J. Lowke (1997), Streamer propagation in air, *J. Phys. D: Appl. Phys.*, *30*, 614–627.

Narcisi, R. S. (1973), Mass Spectrometer Measurements in the Ionosphere, in *Physics and Chemistry of Upper Atmospheres*, *Astrophys. Space Sci. Lib.*, vol. 35, edited by B. M. McCormac, pp. 171–183, D. Reidel, Dordrecht, Holland.

Newsome, R. T., and U. S. Inan (2010), Free-running ground-based photometric array imaging of transient luminous events, *J. Geophys. Res.*, *115*, A00E41, doi:10.1029/2009JA014834.

Pasko, V. P., U. S. Inan, and T. F. Bell (1998), Spatial structure of sprites, *Geophys. Res. Lett.*, *25*, 2123–2126.

Pasko, V. P., U. S. Inan, and T. F. Bell (2000), Fractal structure of sprites, *Geophys. Res. Lett.*, *27*(4), 497–500, doi:10.1029/1999GL010749.

Pasko, V. P., Y. Yair, and C.-L. Kuo (2011), Lightning related transient luminous events at high altitude in the earths atmosphere: Phenomenology, mechanisms and effects, *Space Sci. Rev.*, 287, doi:10.1007/s11214-011-9813-9.

Qin, J., S. Celestin, and V. P. Pasko (2011), On the inception of streamers from sprite halo events produced by lightning discharges with positive and negative polarity, *J. Geophys. Res.*, *116*, A06305, doi:10.1029/2010JA016366.

Qin, J., S. Celestin, and V. P. Pasko (2012a), Formation of single and double-headed streamers in sprite-halo events, *Geophys. Res. Lett.*, *39*, L05810, doi:10.1029/2012GL051088.

Qin, J., S. Celestin, and V. P. Pasko (2012b), Minimum charge moment change in positive and negative cloud to ground lightning discharges producing sprites, *Geophys. Res. Lett.*, *39*, L22801, doi:10.1029/2012GL053951.

Rayment, S. W., and J. L. Moruzzi (1978), Electron detachment studies between O- ions and nitrogen, *Int. J. Mass Spectrom. Ion Process.*, *26*(3), 321–326, doi:10.1016/0020-7381(78)80033-3.

Saba, M. M. F., O. Pinto, Jr., and M. G. Ballarotti (2006), Relation between lightning return stroke peak current and following continuing current, *Geophys. Res. Lett.*, *33*(23), L23807, doi:10.1029/2006GL027455.

Saba, M. M. F., W. Schulz, T. A. Warner, L. Z. S. Campos, C. Schumann, E. P. Krider, K. L. Cummins, and R. E. Orville (2010), High-speed video observations of positive lightning flashes to ground, *J. Geophys. Res.*, *115*, D24201, doi:10.1029/2010JD014330.

Sagalyn, R. C., and H. K. Burke (1985), Fair weather electricity, in *Handbook of Geophysics and the Space Environment*, edited by A. S. Jursa, pp. 20–1, US Air Force Geophysics Laboratory, Air Force Systems Command, United States Air Force.

Sato, M., Y. Takahashi, A. Yoshida, and T. Adachi (2008), Global distribution of intense lightning discharges and their seasonal variations, *J. Phys. D: Appl. Phys.*, *41*(23), 234011, doi:10.1088/0022-3727/41/23/234011.

Sentman, D. D., E. M. Wescott, D. L. Osborne, D. L. Hampton, and M. J. Heavner (1995), Preliminary results from the Sprites94 campaign: Red sprites, *Geophys. Res. Lett.*, *22*, 1205–1208.

Sentman, D. D., H. C. Stenbaek-Nielsen, M. G. McHarg, and J. S. Morrill (2008), Plasma chemistry of sprite streamers, *J. Geophys. Res.*, *113*, D11112.

Stanley, M., P. Krehbiel, M. Brook, C. Moore, W. Rison, and B. Abrahams (1999), High speed video of initial sprite development, *Geophys. Res. Lett.*, *26*, 3201–3204.

Stenbaek-Nielsen, H. C., and M. G. McHarg (2008), High time-resolution sprite imaging: observations and implications, *J. Phys. D: Appl. Phys.*, *41*, 234009.

Stenbaek-Nielsen, H. C., D. R. Moudry, E. M. Wescott, D. D. Sentman, and F. T. S. Sabbas (2000), Sprites and possible mesospheric effects, *Geophys. Res. Lett.*, *27*, 3829–3832.

Stenbaek-Nielsen, H. C., R. Haaland, M. G. McHarg, B. A. Hensley, and T. Kanmae (2010), Sprite initiation altitude measured by triangulation, *J. Geophys. Res.*, *115*, A00E12, doi:10.1029/2009JA014543.

Suzuki, T., Y. Matsudo, T. Asano, M. Hayakawa, and K. Michimoto (2011), Meteorological and electrical aspects of several winter thunderstorms with sprites in the Hokuriku area of Japan, *J. Geophys. Res.-Atmos.*, *116*, D06205, doi:10.1029/2009JD013358.

Swider, W. (1985), Ionized constituents, in *Handbook of Geophysics and the Space Environment*, edited by A. S. Jursa, pp. 21–51, US Air Force Geophysics Laboratory, Air Force Systems Command, United States Air Force.

Taylor, M. J., M. A. Bailey, P. D. Pautet, S. A. Cummer, N. Jaugey, J. N. Thomas, N. N. Solorzano, F. S. Sabbas, R. H. Holzworth, O. Pinto, and N. J. Schuch (2008), Rare measurements of a sprite with halo event driven by a negative lightning discharge over Argentina, *Geophys. Res. Lett.*, *35*(14), L14812, doi:10.1029/2008GL033984.

Usoskin, I., M. Schussler, S. Solanki, and K. Mursula (2005), Solar activity, cosmic rays, and Earth's temperature: A millennium-scale comparison, *J. Geophys. Res.*, *110*, A10102, doi:10.1029/2004JA010946.

Vadislavsky, E., Y. Yair, C. Erlick, C. Price, E. Greenberg, R. Yaniv, B. Ziv, N. Reicher, and A. Devir (2009), Indication for circular organization of column sprite elements associated with Eastern Mediterranean winter thunderstorms, *J. Atmos. Sol.-Terr. Phys.*, *71*(17-18), 1835–1839, doi:10.1016/j.jastp.2009.07.001.

van der Velde, O. A., A. Mika, S. Soula, C. Haldoupis, T. Neubert, and U. S. Inan (2006), Observations of the relationship between sprite morphology and in-cloud lightning processes, *J. Geophys. Res.*, *111*, D15203, doi:10.1029/2005JD006879.

Wait, J. R., and K. P. Spies (1964), Characteristics of the Earth-ionosphere waveguide for VLF radio waves, Tech note 300, National Bureau of Standards: Boulder, Colorado.

Wescott, E. M., D. Sentman, M. Heavner, D. Hampton, W. A. Lyons, and T. Nelson (1998), Observations of 'Columniform' sprites, *J. Atmos. Solar Terr. Phys.*, *60*, 733–740.

Wescott, E. M., H. C. Stenbaek-Nielsen, D. D. Sentman, M. J. Heavner, D. R. Moudry, and F. T. S. Sabbas (2001), Triangulation of sprites, associated halos and their possible relation to causative lightning and micrometeors, *J. Geophys. Res.*, *106*(A6), 10,467–10,478, doi:10.1029/2000JA000182.

Williams, E., E. Downes, R. Boldi, W. Lyons, and S. Heckman (2007), Polarity asymmetry of sprite-producing lightning: A paradox?, *Radio Sci.*, *42*, RS2S17, doi:10.1029/2006RS003488.

Williams, E., C. L. Kuo, J. Bor, G. Satori, R. Newsome, T. Adachi, R. Boldi, A. Chen, E. Downes, R. R. Hsu, W. Lyons, M. M. F. Saba, M. Taylor, and H. T. Su (2012), Resolution of the sprite polarity paradox: The role of halos, *Radio Sci.*, *47*, RS2002, doi:10.1029/2011RS004794.

Zalesak, S. T. (1979), Fully multidimensional flux-corrected transport algorithms for fluids, *J. Comput. Phys.*, *31*, 335–362.